

Counterfactual Modeling with Fine-Tuned LLMs for Health Intervention Design and Sensor Data Augmentation

Shovito Barua Soumma^{1,2}, *Student Member, IEEE*, Asiful Arefeen^{1,2}, Stephanie M. Carpenter¹, Melanie Hingle³, and Hassan Ghasemzadeh¹, *Senior Member, IEEE*

Abstract—Counterfactual explanations (CFEs) provide human-centric interpretability by identifying the minimal, actionable changes required to alter a machine learning model’s prediction. Therefore, CFs can be used as (i) interventions for abnormality prevention and (ii) augmented data for training robust models. we conduct a comprehensive evaluation of CF generation using large language models (LLMs), including GPT-4 (zero-shot and few-shot) and two open-source models—BioMistral-7B and LLaMA-3.1-8B—in both pretrained and fine-tuned configurations. Using the multimodal AI-READI clinical dataset, we assess CFs across three dimensions: intervention quality, feature diversity, and augmentation effectiveness. Fine-tuned LLMs, particularly LLaMA-3.1-8B, produce CFs with high plausibility (up to 99%), strong validity (up to 0.99), and realistic, behaviorally modifiable feature adjustments. When used for data augmentation under controlled label-scarcity settings, LLM-generated CFs substantially restore classifier performance, yielding an average 20% F1 recovery across three scarcity scenarios. Compared with optimization-based baselines such as DiCE, CFNOW, and NICE, LLMs offer a flexible, model-agnostic approach that generates more clinically actionable and semantically coherent counterfactuals. Overall, this work demonstrates the promise of LLM-driven counterfactuals for both interpretable intervention design and data-efficient model training in sensor-based digital health.

Index Terms—Counterfactual explanations, Digital health, Explainable AI, Label Scarcity, Large Language Model (LLM)

Impact Statement—SenseCF fine-tunes an LLM to generate valid, representative counterfactual explanations and supplement minority class in an imbalanced dataset for improving model training and boosting model robustness and predictive performance.

I. INTRODUCTION

ACCURATE and interpretable predictions from machine learning (ML) models are increasingly vital in healthcare

¹College of Health Solutions, Arizona State University, Phoenix, AZ 85004, USA. Emails: {shovito, aarefeen, stephanie.m.carpenter, hghasemz}@asu.edu.

²School of Computing and Augmented Intelligence, Arizona State University, Tempe, AZ 85281, USA.

³School of Nutritional Sciences and Wellness, University of Arizona, Tucson, AZ 85721, USA. Email: hinglem@arizona.edu.

This work was supported in part by the National Science Foundation (NSF) under Grant IIS-2402650. A. Arefeen was supported in part by the National Institute of Diabetes and Digestive and Kidney Diseases (NIDDK) of the National Institutes of Health (NIH) under Award T32DK137525. The content is solely the responsibility of the authors and does not necessarily represent the official views of the NSF or NIH.

applications such as disease risk forecasting and sleep efficiency estimation using physiological and sensor data. While these models excel at outcome prediction, they often fall short in guiding actionable interventions to reverse adverse outcomes—specially in black-box settings.

Counterfactual explanations (CFEs) offer a powerful approach for model interpretability by identifying the minimal, actionable changes needed to reverse an undesirable prediction, a concept first formalized in the seminal work of Wachter et al [1]. Subsequent surveys and methodological frameworks [2]–[4] have emphasized CFs’ central role in actionable recourse, feasibility constraints, and user-centered interpretability. Traditional optimization-driven CF methods such as DiCE [5], CFNOW [6], and NICE [7] often require access to model gradients or internal structure, limiting their real-world applicability and frequently struggling with categorical coherence or clinically plausible modifications. In contrast, large language models (LLMs) provide a promising alternative: leveraging zero- and few-shot prompting, they can generate realistic, semantically consistent counterfactuals using only input–output context [8], [9]. This paradigm not only eliminates the dependency on gradients or model access but also opens the door for scalable, human-centered explanations across diverse datasets.

Recent work highlights that LLMs possess strong innate counterfactual reasoning abilities even without task-specific fine-tuning [9]–[12], building on earlier foundations showing that counterfactual reasoning supports actionable model transparency [1]–[4]. However, their application to structured and multimodal health data—where features arise from heterogeneous physiological, behavioral, and environmental sensors—remains largely underexplored. Beyond interpretability, counterfactual explanations also serve as label-flipping synthetic samples that generate corner cases and enhance model robustness in imbalanced medical datasets, advancing prior work demonstrating the utility of counterfactuals for recourse, robustness, and data augmentation [13]. When used for augmentation, CFs introduce controlled perturbations that preserve the underlying data manifold while enriching decision-boundary diversity, improving resilience in low-data clinical scenarios. Although optimization-based CF approaches have shown effectiveness in decision-support settings [5], [6], they often struggle with categorical constraints, nonlin-

ear physiological dependencies, and plausible semantic adjustments—limitations that LLMs can mitigate through their contextual reasoning and stronger distributional priors [7], [10].

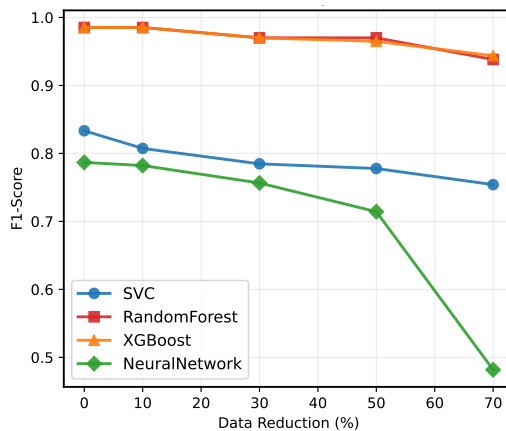


Fig. 1. F1-Score Decline Across Models as Training Data is Reduced.

However, several critical gaps persist in the current literature: first, the effectiveness of LLM-based CFs have not been comprehensively evaluated on large, multimodal clinical datasets; second, standardized evaluation metrics comparing optimization-based and generative approaches remain limited; third, CFs' potential as data augmenters in healthcare scenarios remains underexplored. As illustrated in Fig. 1, all classifiers experience marked declines in F1-score under increasing data reduction, highlighting the vulnerability of standard models to label scarcity and motivating the need for principled synthetic augmentation via LLM-generated counterfactuals.

To address these gaps, we introduce a systematic evaluation of LLM-generated counterfactuals using zero-shot, few-shot, pretrained, and fine-tuned models across the multimodal AI-READI clinical dataset. This paper extends our earlier work, SenseCF [9], which focused primarily on GPT-4o based prompting, by incorporating a broader suite of open source LLMs and performing a more comprehensive assessment of their counterfactual capabilities. Our contributions extend beyond existing LLM-focused studies that primarily evaluate natural language processing (NLP) tasks, providing a rigorous and quantitative comparison in multimodal clinical settings [10], [11]. In this work, (i) We systematically compare GPT-4o with two open-source LLMs (BioMistral-7B and LLaMA-3.1-8B) evaluated in both pretrained and fine-tuned configurations. We assess their performance across three core dimensions: (a) actionable intervention quality, (b) feature diversity and realism, and (c) data augmentation effectiveness under controlled label-scarcity scenarios. (ii) We further benchmark their plausibility, diversity, and impact on model performance against state-of-the-art baselines.

To the best of our knowledge, this is the first study¹ to fine-tune LLMs and explore them as counterfactual generators for both actionable explanation and augmentation in sensor-driven health contexts, moving toward AI systems that can inform not just prediction, but intervention.

II. MATERIALS AND METHODS

In this section, we detail our approach for generating and evaluating counterfactual explanations (CFs) using large language models (LLMs). As illustrated in Fig 3 and Fig 2, our methodology aims at: (1) producing actionable counterfactual (CF) interventions by reversing the predictions of trained ML models, and (2) leveraging these CFs as augmented training data to enhance model robustness, specifically under label scarcity.

A. Study Design

We represent our input data as a set of tuples (x_i, y_i) , where $x_i \in X$ is a feature vector representing either clinical or physiological data and $y_i \in \{0, 1\}$ denotes the ground truth label. A trained predictive model $f(\cdot)$ outputs predictions $\hat{y}_i = f(x_i)$. Our preprocessing stage (discussed in Section II-C) transforms raw data into structured, tabular feature vectors suitable for prompting the LLM.

1) *Counterfactual Generation*: To generate counterfactuals, we used three LLM families under four generative modes:

- 1) **GPT-4o**: Zero-shot (ZS) and few-shot (FS) prompting
- 2) **BioMistral-7B**: Zero-shot and fine-tuned (FT) on the structured training data
- 3) **LLaMA-3.1-8B**: Zero-shot and fine-tuned on the structured training data

Problem Formulation: Given a feature vector x_i and the prediction \hat{y}_i , each LLM generates a modified vector x'_i , where the model's prediction changes from \hat{y}_i to a desired opposite outcome $y_i \neq \hat{y}_i$. We also explicitly constrain the LLM from altering immutable or clinically fixed features (e.g., age, sex, or medication type), ensuring that generated counterfactuals remain actionable and plausible within domain constraints. The generation of CFs can be described as:

$$x'_i = \text{LLM}(x_i, \text{prompt}), \quad \text{s.t. } f(x'_i) \neq f(x_i)$$

The instructional prompt explicitly constrains LLM to minimally alter feature values to achieve a realistic and actionable counterfactual, ensuring the plausibility and feasibility of generated CFs. This multi-model setup enables us to compare the semantic precision, boundary awareness, and distributional alignment of counterfactuals produced by proprietary vs. open-source models and by zero-shot prompting vs. supervised fine-tuning.

2) *Intervention, Diversity and Data Augmentation*: Generated CFs serve three purposes in our analysis:

(i) **Intervention**: We assess whether CFs provide actionable and clinically meaningful adjustments to move a sample from an undesired label (e.g., stressed, disease-positive) to a desirable outcome. Validity, sparsity, and plausibility metrics quantify intervention realism.

(ii) **Diversity**: We also analyze how different LLMs modify feature distributions, highlighting whether fine-tuned models produce semantically grounded and structurally consistent CFs.

(iii) **Data Augmentation**: CFs that successfully alter the model prediction are added to the training dataset to form an augmented set:

$$X_{\text{aug}} = X \cup \{(x'_i, y'_i) \mid f(x'_i) \neq f(x_i)\}$$

¹A preliminary version of this work has been reported [9].

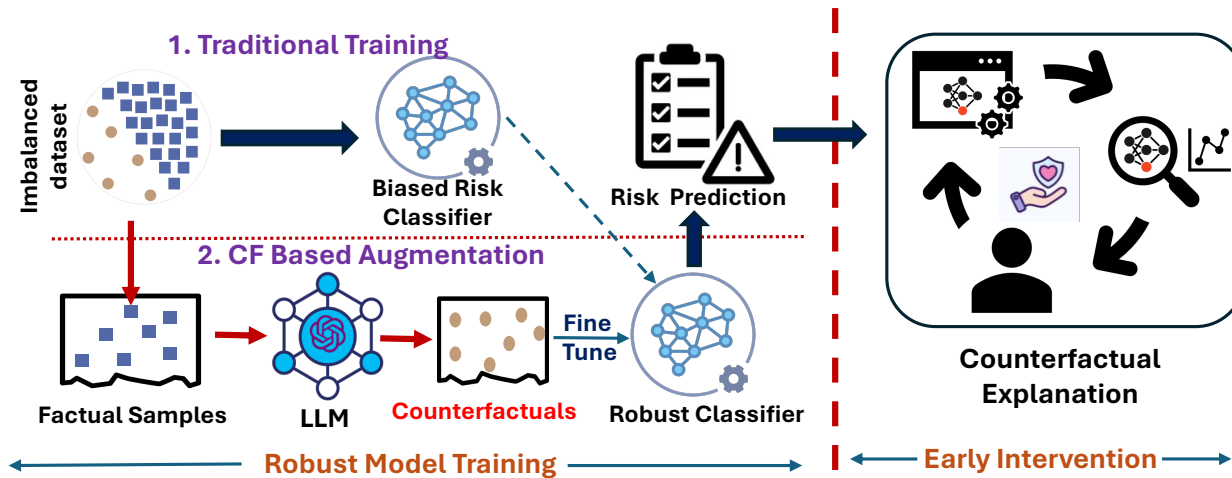


Fig. 2. SenseCF pipeline: LLM-generated counterfactuals are used both for augmenting imbalanced training data (left) and for model interpretability (right).

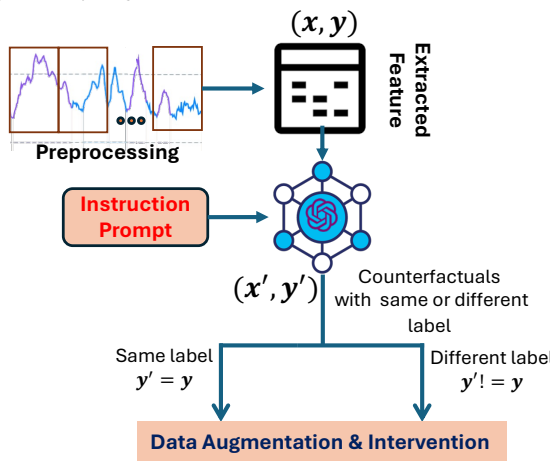


Fig. 3. Counterfactual generation using LLMs from sensor-derived features.

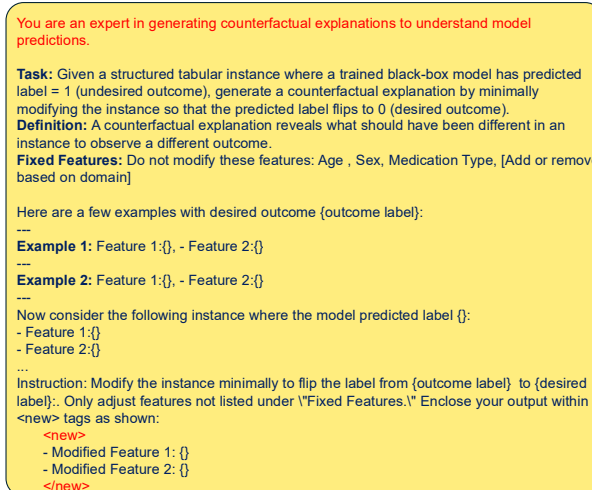


Fig. 4. Prompt template for counterfactual generation.

We evaluate the impact of CF augmentation under three different label-scarcity settings (Positive-Class Scarcity, Negative-Class Scarcity, Dual-Class Scarcity) and across multiple augmentation ratios. This allows us to quantify how CF quantity and LLM fine-tuning quality improve downstream classifier

performance.

B. Dataset

AIREADI data: SenseCF utilizes the publicly available AIREADI Flagship Dataset [14], [15], a resource developed to support artificial intelligence and machine-learning research in Type 2 Diabetes Mellitus (T2DM). The dataset contains information from 1,067 participants recruited across three U.S. locations: the University of Alabama at Birmingham (UAB), the University of California San Diego (UCSD), and the University of Washington (UW). AIREADI includes individuals both with and without T2DM, with careful balancing across demographic groups and diabetes status. Participants fall into four categories: healthy controls, individuals with prediabetes, individuals with T2DM treated with oral agents, and individuals with T2DM using insulin.

A major strength of the dataset is its rich multimodal composition. Each participant was monitored over a ten-day period using multiple wearable sensors: a Dexcom G6 continuous glucose monitor for frequent glucose measurements, a Garmin Vivosmart 5 for physical activity and heart-rate-variability-derived stress indices, and an Anura environmental sensor capturing factors such as air quality and temperature. Additional components include self-reported surveys, clinical examinations, and retinal images. Daily step counts were obtained via an accelerometer, with occasional missing values due to device charging.

C. Preprocessing and Feature Extraction

Figure 5 illustrates the overall preprocessing pipeline used in this study. To avoid data leakage across samples from the same individual, we perform the train-test split at the patient level, assigning 80% of patients to the training set and the remaining 20% to the test set. This ensures that no temporal windows, physiological patterns, or behavioral characteristics from a given patient appear in both sets, thereby preserving the integrity of model evaluation.

From each night, the *Awake*, *Light Sleep*, *Deep Sleep* and *REM Sleep* percentages are computed. A two-hour long moving

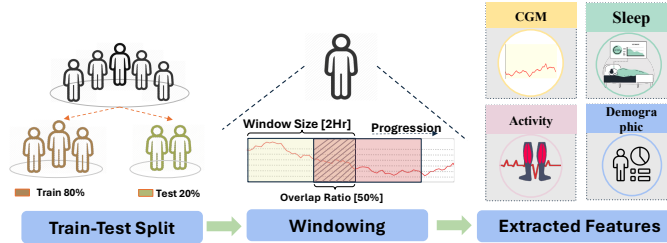


Fig. 5. Overview of the feature extraction pipeline. Patients are first split into train and test sets to avoid data leakage. A two-hour sliding window with 50% overlap is applied to continuous signals, followed by extraction of sleep, CGM, activity, and demographic features.

window is used to extract *mean step counts*, *mean glucose level*, *number of hyperglycemic events*, percentage of time-in-range for glucose levels (*%TIR*). Based on high (mean daily stress > 75) and moderate stress (mean daily stress 75) levels [16], the target label is set. Therefore, a total of 12 features, including 4 immutable features: *Age*, *Gender*, *Medication* and *Patient Subgroup*, are used to classify a sample for high/moderate stress and generate the CFEs for supplementing the minority class.

D. Experimental Setup

All experiments were conducted using a single NVIDIA A100 GPU (40 GB), which provides sufficient memory bandwidth and tensor-core acceleration for finetuning 7–8B parameter large language models. We fine-tuned two models: Llama-3.1-8B-Instruct and BioMistral-7B, using parameter-efficient LoRA adaptation rather than full-model training to reduce computational cost and prevent catastrophic forgetting of medical knowledge. Both models were trained for 2 epochs, as we found this to provide the best trade-off between learning stability and overfitting; additional epochs tended to yield diminishing returns on validation loss. We applied 4-bit NF4

TABLE I. Training Configuration for LLM Finetuning

Component	Setting
GPU	NVIDIA A100
Models	Llama-3.1-8B, BioMistral-7B
Finetuning Strategy	LoRA (PEFT)
LoRA Rank (r)	16
LoRA Alpha	32
LoRA Dropout	0.03
Quantization	4-bit NF4 (BitsAndBytes)
Epochs	2
Batch Size	4 (effective 16 with GA=4)
Learning Rate	2e-4
Max Sequence Length	512 tokens
Precision	FP16
Eval Frequency	Every 50 steps
Checkpoint Frequency	Every 100 steps

quantization (BitsAndBytes) only to the Llama-3.1-8B model in order to substantially reduce its memory footprint on the A100 GPU. LLaMA models have larger attention projections and higher activation memory compared to BioMistral-7B, making them more memory-intensive during finetuning. Quantizing LLaMA to NF4 allows the model to fit comfortably

in GPU memory, enables larger effective batch sizes, and avoids out-of-memory (OOM) errors during training—while preserving model quality and maintaining stable optimization under LoRA.

E. Baselines

We have identified the following techniques to compare against SenseCF.

(i) **DiCE** [5] generates a diverse set of CFs to maximize variability across solutions while also optimizing for proximity, and feasibility across local regions of the decision boundary.

(ii) **CFNOW** [6] is a model-agnostic method that employs a two-step search algorithm to explore the search space and generate valid and minimal CFs.

(iii) **NICE** [7] iteratively constructs CFs by replacing feature values with those from the nearest instance having a different prediction

F. Evaluation Metrics

We assess the CFs using some standard metrics found in the literature:

Validity assesses whether the produced CFs genuinely belong to the desired class [17]. High validity indicates the technique’s effectiveness in generating valid CF examples.

$$\text{validity} = \frac{\#|f(X_T^*) \neq f(X_T)|}{\|CF\|}$$

Distance between the CF and the factual sample is calculated from the L_2 normalized distance of the continuous features and the hamming distance of the categorical features [3].

Sparsity is the average number of feature changes per CF [18]. A low sparsity ensures better user understanding of the CFs.

$$\text{sparsity} = \frac{\sum_{X_T^* \in CF} \sum_{i=1}^d \mathbb{1}(x_T^{*i} \neq x_T^i)}{\|CF\|} \quad (1)$$

Plausibility quantifies the fraction of explanations that fall within the feature ranges derived from the data [19]—

$$\text{plausibility} = \frac{\sum_{X_T^* \in CF} \mathbb{1}(\text{dist}(X_T^*) \subseteq \text{dist}(X))}{\|CF\|}$$

where, $\text{dist}(X_T^*)$ and $\text{dist}(X)$ represent the distribution of feature values in the CF instances X_T^* and in the training data, respectively. $\|CF\|$ is the total number of CF instances.

III. RESULTS

Our evaluation highlights the dual role of LLM-generated CFs as highly plausible interventions and as impactful data augmenters for robust model training in digital health contexts.

A. Intervention

The counterfactual intervention in Table II illustrates how LLMs can propose clinically meaningful and physiologically grounded modifications for a high-stress patient. In this example, the model identifies low deep sleep, moderate REM sleep, elevated glucose (210.8 mg/dL), and low activity as major contributors to the stress prediction.

Condition

An 81-year-old patient labeled as “**stressed**” showed low deep sleep (30.1%), moderate REM (15.4%), high blood glucose (210.8 mg/dL), and limited activity (5.95 steps). Stress level was high (85.25), with poor glucose control (TIR: 12.5%, 1 hyper event).

Intervention

The LLM suggests **increasing deep sleep** to ↑35% and **REM sleep** to ↑20%, which could help reduce physiological and emotional stress. It also recommends **lowering blood glucose** from 210.8 to ↓180 mg/dL, aligning with better metabolic control. These changes reflect clinically actionable strategies such as sleep hygiene improvement and tighter glucose management.

TABLE II. Example of LLM-suggested counterfactual intervention for a high-stress patient

Method	Class 0 Metrics				Class 1 Metrics			
	Validity ↑	Distance ↓	Sparsity ↓	Plausibility ↑	Validity ↑	Distance ↓	Sparsity ↓	Plausibility ↑
DiCE	0.67	0.2	2.27	100	0.58	0.41	2.4	99
CFNOW	0.85	0.1	2.9	100	0.84	0.25	3	99
NICE	0.44	0.02	1.12	33	0.53	0.04	1.31	35
GPT-4 (ZS)	0.91	1.1	3.6	85	0.89	1.5	3.8	82
GPT-4 (FS)	0.99	1.2	4.4	99	0.92	1.82	4	96
BioMistral	0.51	1.4	5.2	77	0.47	1.5	4.1	70
Llama	0.62	1.6	4.6	91	0.68	1.3	3.8	78
BioMistral*	0.93	0.92	2.27	90	0.91	1.0	2.1	95
Llama*	0.99	0.41	1.8	99	0.98	0.2	1.9	99

TABLE III. Evaluating CFs on AI-READI Dataset for Class 0 and Class 1. ZS: Zero-shot, FS: Few-shot, *: Fine-tuned, Red: best, Blue: second-best.

Table III provides a comparison of counterfactual quality across baseline optimization methods, GPT-4, and open-source LLMs. While traditional methods such as DiCE, CFNOW, and NICE achieve strong plausibility and occasionally lower distances, they often propose unrealistic or non-actionable feature shifts. GPT-4 performs reliably in both zero-shot and few-shot modes, but its counterfactuals still exhibit larger feature deviations than desired for sensor-derived tabular data.

Fine-tuned BioMistral-7B and LLaMA-3.1-8B substantially improve validity, sparsity, and distance relative to their pre-trained versions—showing gains of 20–40% points in validity and reductions of more than 50% in feature distance. Although fine-tuned LLMs do not always outperform every state-of-the-art baseline across all metrics, they remain highly competitive overall. Importantly, fine-tuned LLaMA provides the strongest balance across metrics, achieving near-perfect validity with minimal, clinically realistic modifications.

Unlike optimization-based methods (e.g., DICE, CFNOW), which rely on access to model internals, our LLM-based approach generates CFs in a model-agnostic fashion while remaining interpretable and actionable.

Feature Diversity: The radar plot (Fig 6) highlights important differences in actionability and realism across counterfactual generation methods. Traditional CF methods such as DICE and CFNOW often propose large shifts in physiological features—specially sleep-stage percentages and total sleep duration—that are not immediately modifiable in real-life settings and therefore have lower practical utility. NICE performs better by recommending smaller, more localized changes, but it still occasionally alters features like REM or deep sleep that individuals cannot directly control in the short

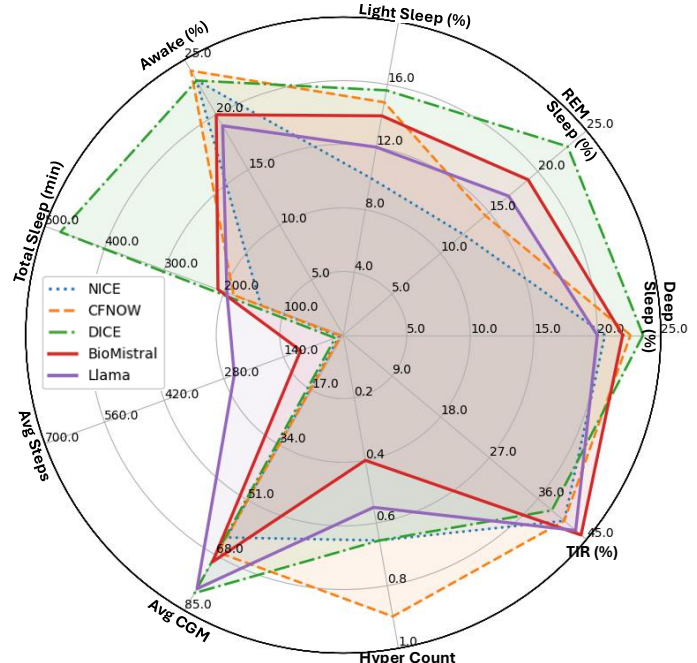


Fig. 6. Feature diversity in the generated CFs for AI-READI data. Avg: Average, Hyper: No. of hyperglycemia

term. In contrast, the fine-tuned BioMistral and Llama models produce counterfactuals concentrated around *highly actionable variables*, such as average steps, glucose levels (Avg CGM, TIR%), and hyperglycemia frequency—factors that can be modified through short-term behavioral or treatment adjustments. This shift toward modifiable lifestyle and metabolic variables makes the LLM-based counterfactuals more clinically realistic and better aligned with interventions that individuals

TABLE IV. Performance Impact of LLM-Generated Counterfactuals Under Three Label-Scarcity Scenarios. Baseline performance is measured on the full training set. Negative values indicate the performance drop after undersampling. CF-added rows report the improvement relative to the reduced dataset.

Scenario	Method	ACC	PRE	REC	F1	AUC
Baseline (Using Full Training Set)	NN	71.8	0.68	0.68	0.68	0.78
Scenario A — Positive-Class Undersampling (Class 1 Reduced by 50%)						
Model trained on reduced data	NN	-12.87% \downarrow	-11.76% \downarrow	-16.18% \downarrow	-14.71% \downarrow	-14.10% \downarrow
	BioMistral	7.10% \uparrow	5.00% \uparrow	8.77% \uparrow	6.90% \uparrow	7.46% \uparrow
	LLaMA	8.54% \uparrow	6.67% \uparrow	10.53% \uparrow	8.62% \uparrow	7.46% \uparrow
CF Added (Recovery over Reduced)	GPT-4	10.29% \uparrow	10.00% \uparrow	12.28% \uparrow	12.07% \uparrow	11.94% \uparrow
	BioMistral*	14.93% \uparrow	18.33% \uparrow	22.81% \uparrow	20.69% \uparrow	20.90% \uparrow
	LLaMA*	21.00% \uparrow	20.00% \uparrow	24.56% \uparrow	22.41% \uparrow	25.37% \uparrow
Scenario B — Negative-Class Undersampling (Class 0 Reduced by 50%)						
Model trained on reduced data	NN	-10.72% \downarrow	-8.82% \downarrow	-10.29% \downarrow	-10.29% \downarrow	-12.82% \downarrow
	BioMistral	4.52% \uparrow	1.61% \uparrow	1.64% \uparrow	1.64% \uparrow	4.41% \uparrow
	LLaMA	5.93% \uparrow	3.23% \uparrow	3.28% \uparrow	3.28% \uparrow	5.88% \uparrow
CF Added (Recovery over Reduced)	GPT-4	6.86% \uparrow	4.84% \uparrow	4.92% \uparrow	4.92% \uparrow	8.82% \uparrow
	BioMistral*	14.82% \uparrow	14.52% \uparrow	13.11% \uparrow	14.75% \uparrow	20.59% \uparrow
	LLaMA*	17.16% \uparrow	16.13% \uparrow	16.39% \uparrow	16.39% \uparrow	23.53% \uparrow
Scenario C — Dual-Class Undersampling (Both Classes Reduced by 50%)						
Model trained on reduced data	NN	-11.14% \downarrow	-10.29% \downarrow	-13.24% \downarrow	-11.76% \downarrow	-14.10% \downarrow
	BioMistral	4.55% \uparrow	1.64% \uparrow	3.39% \uparrow	1.67% \uparrow	4.48% \uparrow
	LLaMA	5.90% \uparrow	4.92% \uparrow	6.78% \uparrow	5.00% \uparrow	7.46% \uparrow
CF Added (Recovery over Reduced)	GPT-4	6.27% \uparrow	4.92% \uparrow	5.08% \uparrow	5.00% \uparrow	8.96% \uparrow
	BioMistral*	15.99% \uparrow	16.39% \uparrow	16.95% \uparrow	16.67% \uparrow	22.39% \uparrow
	LLaMA*	21.47% \uparrow	19.67% \uparrow	22.03% \uparrow	20.00% \uparrow	26.87% \uparrow

can adopt immediately. Overall, the Llama model generates the most actionable and plausible counterfactual recommendations, avoiding unrealistic alterations to intrinsic sleep architecture while still achieving high validity in flipping the prediction.

B. Augmentation

1) *Performance Recovery*: Table IV summarizes the impact of LLM-generated counterfactual samples on classifier performance under three controlled label-scarcity settings. We first trained a neural network on the full training set to establish a baseline. Next, we constructed three undersampling scenarios: (1) Positive-Class Scarcity (Class 1 undersampled), (2) Negative-Class Scarcity (Class 0 undersampled), and (3) Dual-Class Scarcity (both classes undersampled). In each case, removing 50% of the samples from the targeted class resulted in a substantial performance drop across all metrics, as reflected by negative deltas relative to the baseline neural network. To recover the lost information, we generated counterfactual samples using several LLMs (BioMistral-7B, LLaMA-3.1-8B, and GPT-4o) in both zero-shot and fine-tuned configurations, and added only the counterfactuals corresponding to the class that was undersampled. The “CF Added” rows report the performance recovery relative to the reduced-data model, showing that fine-tuned LLMs consistently provide the largest improvement, with fine-tuned LLaMA delivering the strongest gains across all three scarcity scenarios.

LLaMA-3.1-8B (FT) restores more than 22% of F1 in the positive-class scarcity setting and roughly 20% under

dual-class scarcity—fully reversing the degradation introduced by undersampling. Even in the more challenging negative-class scarcity case, fine-tuned LLMs recover 16–17% of F1, clearly outperforming their zero-shot counterparts. These large percentage-point gains highlight the strong corrective effect of CF-based augmentation when guided by fine-tuned LLMs.

2) *Effect of Augmentation Ratio*: Figure 7 further explores how the amount of counterfactual augmentation influences performance by varying the augmentation ratio from 20% to 100%. Each subplot begins with the reduced-data model in Scenario A, B, or C, where the neural network exhibits markedly degraded performance due to undersampling; this is shown as the horizontal dashed baseline in Figure 7 (A-C). Starting from these weakened models, we incrementally add different quantities of LLM-generated counterfactuals and observe how performance recovers as augmentation increases. Across all three scarcity scenarios, the F1 score improves steadily as more counterfactuals are injected into the training set. The effect is most pronounced for the fine-tuned LLaMA-3.1-8B and BioMistral-7B models, which show clear monotonic gains and achieve the highest F1 scores at large augmentation ratios.

Zero-shot LLMs (dashed lines) still provide measurable improvement over the undersampled baseline, but their gains plateau earlier, suggesting limited ability to mimic the true class manifold without task-specific adaptation. Another consistent observation is that Positive-Class Scarcity and Dual-Class Scarcity benefit more strongly from CF augmentation than Negative-Class Scarcity, indicating that the model is par-

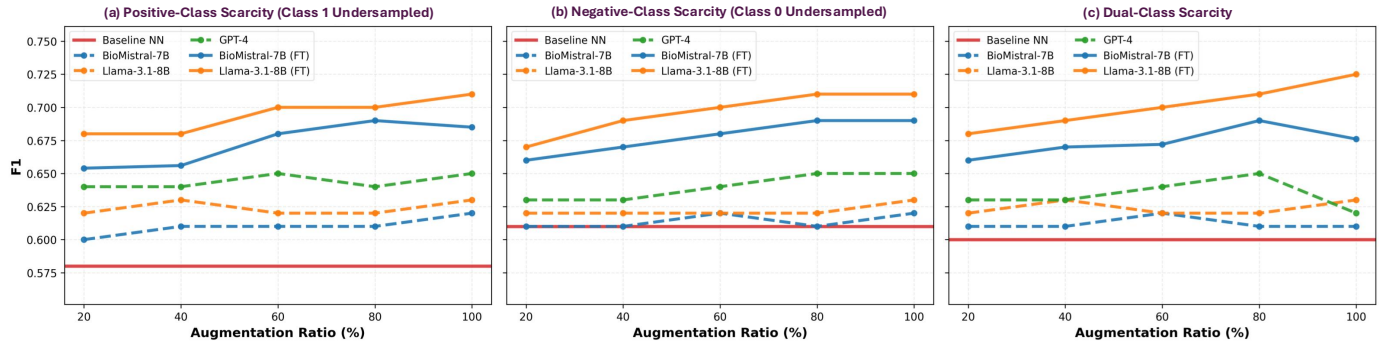


Fig. 7. Impact of LLM-Generated Counterfactual Augmentation Under Class-Specific Label Scarcity

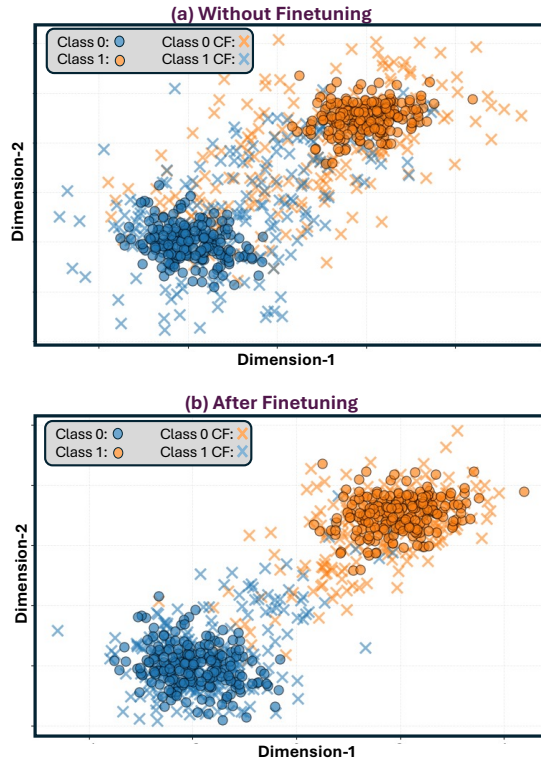


Fig. 8. Latent Space Distribution of Factual and Counterfactual Samples Generated by LLaMA-3.1-8B on the AI-READI Dataset (Before vs. After Fine-Tuning). The amount of overlap between two classes is much lesser in the dataset augmented using fine-Tuned LLM.

ticularly sensitive to missing minority-class examples. Overall, the F1 curves demonstrate that counterfactuals function as an effective and controllable data augmenter, with augmentation magnitude and LLM fine-tuning both playing significant roles in performance recovery.

C. Ablation Study

Fine-tuning LLaMA-3.1-8B leads to markedly improved counterfactual behavior, as shown in Figure 8. Using a randomly selected subset of 200 factual samples, the zero-shot model generates diffused and often misaligned CFs; the fine-tuned model produces CFs that cluster tightly within the appropriate class region and maintain local structural coherence. This improved spatial organization highlights the effectiveness

of finetuning in producing plausible, semantically meaningful, and distribution-consistent counterfactuals.

IV. DISCUSSION

This study presents the first systematic evaluation of LLM-generated counterfactuals for intervention design and data augmentation in sensor-derived health datasets. We evaluate multiple LLM families—GPT-4o, BioMistral-7B, and LLaMA-3.1-8B—in both pretrained and fine-tuned configurations, demonstrating that fine-tuned LLaMA achieves an average 19.9% F1 recovery across three scarcity conditions when 50% of labels are removed. This represents a substantial improvement in classifier robustness under label scarcity while providing interpretable, domain-aligned explanations that traditional CF methods cannot offer.

Our comparative analysis reveals a critical distinction between LLM-based and optimization-based approaches: while traditional methods (DiCE, CFNOW, NICE) frequently modify clinically intractable features such as sleep architecture, fine-tuned LLMs prioritize actionable variables—average steps, glucose metrics (Avg CGM, TIR%), and hyperglycemia frequency—that reflect realistic behavioral interventions. Latent-space visualizations confirm that fine-tuned LLaMA produces semantically coherent CFs aligned with the target class manifold, addressing a key limitation of existing methods.

A. Clinical Implications

These findings highlight the potential for LLM-generated counterfactuals to support personalized health guidance. By suggesting small, clinically plausible adjustments grounded in sensor-derived physiology, CFs can help identify early behavioral or metabolic interventions for individuals at risk. Moreover, CF-based augmentation offers a scalable alternative to collecting more sensor data, helping improve classifier robustness in health settings where labeled data are scarce.

B. Dataset & Limitation

We selected the AI-READI dataset because publicly available clinical datasets suitable for LLM fine-tuning on structured tabular health features are extremely limited. Most open-source biomedical datasets are too small, lack multimodal coverage, or contain insufficient feature richness for effective

LLM alignment. AI-READI, by contrast, offers a large, well-curated combination of CGM, activity, sleep, demographic, and stress features—making it one of the few datasets capable of supporting robust LLM fine-tuning and CF evaluation.

Despite strong overall performance, fine-tuned LLMs do not outperform all state-of-the-art CF baselines across every metric, particularly in distance or sparsity for certain classes. Some CFs may still exceed clinically achievable ranges, and fine-tuning requires labeled data that may be scarce for some conditions. Finally, our work is limited to structured tabular features and does not yet incorporate multimodal raw sensor streams or clinical text.

C. Future Directions

Several promising avenues remain for improving LLM-based counterfactual reasoning. First, integrating LLMs directly into the machine learning training loop could enable iterative, CF-guided model updates (“LLM-in-the-loop learning”). Second, incorporating clinical knowledge graphs or causal structures into the fine-tuning pipeline may reduce unrealistic or physiologically implausible feature changes. Third, expanding beyond tabular data to multimodal LLMs could enable CF generation from raw sensor traces, free-text clinical notes, or imaging. Lastly, deploying CF-driven augmentation in real-world digital health ecosystems may help assess the longer-term impact of CF-based guidance on early intervention and patient outcomes.

V. CONCLUSION

In this work, we introduce a novel framework for generating CFs using large language models (LLMs) and extend it to evaluate both proprietary and open-source models across multiple generative settings. Our results show that LLM-generated counterfactuals are semantically coherent, clinically plausible, and capable of improving downstream robustness when used for data augmentation—restoring, on average, 20% F1 under severe label scarcity. Fine-tuned LLaMA and BioMistral models, in particular, produce compact and actionable CFs that outperform their pretrained counterparts and remain competitive with state-of-the-art optimization methods.

To the best of our knowledge, this is the first systematic exploration of LLM-based CFs in sensor-driven data under both zero- and few-shot settings. We believe this opens a promising direction for integrating generative AI into trustworthy, intervention-oriented healthcare ML pipelines.

REFERENCES

- [1] S. Wachter, B. D. Mittelstadt, and C. Russell, “Counterfactual explanations without opening the black box: Automated decisions and the gdpr,” *Cybersecurity*, 2017.
- [2] R. Guidotti, A. Monreale, F. Turini, D. Pedreschi, and F. Giannotti, “A survey of methods for explaining black box models,” *ACM Computing Surveys (CSUR)*, vol. 51, pp. 1 – 42, 2018.
- [3] A.-H. Karimi, B. Scholkopf, and I. Valera, “Algorithmic recourse: from counterfactual explanations to interventions,” *Proceedings of the 2021 ACM Conference on Fairness, Accountability, and Transparency*, 2020.
- [4] A.-H. Karimi, G. Barthe, B. Balle, and I. Valera, “Model-agnostic counterfactual explanations for consequential decisions,” *ArXiv*, vol. abs/1905.11190, 2019.
- [5] R. K. Mothilal, A. Sharma, and C. Tan, “Explaining machine learning classifiers through diverse counterfactual explanations,” in *Proceedings of the 2020 Conference on Fairness, Accountability, and Transparency*, 2020, pp. 607–617.
- [6] R. M. B. de Oliveira, K. Sørensen, and D. Martens, “A model-agnostic and data-independent tabu search algorithm to generate counterfactuals for tabular, image, and text data,” *European Journal of Operational Research*, 2023.
- [7] D. Brughmans and D. Martens, “Nice: an algorithm for nearest instance counterfactual explanations,” *Data Mining and Knowledge Discovery*, pp. 1–39, 2021.
- [8] B. Mann, N. Ryder, M. Subbiah, J. Kaplan, P. Dhariwal, A. Neelakantan, P. Shyam, G. Sastry, A. Askell, S. Agarwal *et al.*, “Language models are few-shot learners,” *arXiv preprint arXiv:2005.14165*, vol. 1, p. 3, 2020.
- [9] S. B. Soumma, A. Arefeen, S. M. Carpenter, M. Hingle, and H. Ghasemzadeh, “SenseCF: LLM-prompted counterfactuals for intervention and sensor data augmentation,” in *IEEE-EMBS International Conference on Body Sensor Networks 2025*, 2025. [Online]. Available: <https://openreview.net/forum?id=8qqMeF9EmT>
- [10] A. Bhattacharjee, R. Moraffah, J. Garland, and H. Liu, “Zero-shot LLM-guided Counterfactual Generation: A Case Study on NLP Model Evaluation,” in *2024 IEEE International Conference on Big Data (BigData)*. Los Alamitos, CA, USA: IEEE Computer Society, Dec. 2024, pp. 1243–1248. [Online]. Available: <https://doi.ieeecomputersociety.org/10.1109/BigData62323.2024.10825537>
- [11] Y. Li, M. Xu, X. Miao, S. Zhou, and T. Qian, “Prompting large language models for counterfactual generation: An empirical study,” in *Proceedings of the 2024 Joint International Conference on Computational Linguistics, Language Resources and Evaluation (LREC-COLING 2024)*, N. Calzolari, M.-Y. Kan, V. Hoste, A. Lenci, S. Sakti, and N. Xue, Eds. Torino, Italia: ELRA and ICCL, May 2024, pp. 13 201–13 221. [Online]. Available: <https://aclanthology.org/2024.lrec-main.1156/>
- [12] Y. Chen, V. K. Singh, J. Ma, and R. Tang, “Counterbench: A benchmark for counterfactuals reasoning in large language models,” *ArXiv*, vol. abs/2502.11008, 2025.
- [13] C. Russell, “Efficient search for diverse coherent explanations,” *Proceedings of the Conference on Fairness, Accountability, and Transparency*, 2019.
- [14] P. M. <http://orcid.org/0000-0001-6343-2140> Drolet Caroline 4 <http://orcid.org/0000-0003-2287-4190> Lucero Abigail 8 Matthies Dawn 7 <http://orcid.org/0009-0003-4909-6058> Pittock Hanna 3 Watkins Kate 3 York Brittany 1 and N. P. S. W. X. 11, “Ai-readi: rethinking ai data collection, preparation and sharing in diabetes research and beyond,” *Nature metabolism*, vol. 6, no. 12, pp. 2210–2212, 2024.
- [15] S. L. Baxter, V. R. de Sa, K. S. Ferryman, P. Jain, C. S. Lee, J. Li-Pook-Than, T. Y. A. Liu, J. P. Owen, B. Patel, Q. Yu, L. M. Zangwill, A. Bahmani, C. G. Chute, J. C. Edberg, S. Hurst, H. Ishikawa, A. Y. Lee, G. McGwin, S. K. McWeeney, C. Nebeker, C. Owlesley, S. J. Singer, R. Adib, M. Adibuzzaman, A. Alavi, C. Ashley, A. Baer, E. Benton, M. Blazes, A. Cohen, B. A. Cordier, K. Crist, C. Cuddy, A. Gasimova, N. Gim, S. S. Hong, T. Kim, W.-C. Lin, J. Mitchell, C. Ngadisastro, V. Patronilo, J. Shaffer, S. Soundarajan, K. Zhao, C. Drolet, A. Lucero, D. S. Matthies, H. Pittock, K. Watkins, B. York, C. E. Amankwa, M. Bangudi, N. Haboudal, S. Hallaj, A. Heinke, L. Huang, F. G. P. Kalaw, A. Karsolia, H. Khazaei, M. Mohammed, K. U. Simpkins, and X. Wang, “Ai-readi: rethinking ai data collection, preparation and sharing in diabetes research and beyond,” *Nature Metabolism*, vol. 6, pp. 2210 – 2212, 2024.
- [16] Garmin, “What do the stress level numbers mean?” <https://support.garmin.com/en-US/?faq=WT9BmhjacO4ZpxbCc0EKn9>, accessed: 2025-12-02.
- [17] F. Hamman, E. Noorani, S. Mishra, D. Magazzeni, and S. Dutta, “Robust counterfactual explanations for neural networks with probabilistic guarantees,” in *International Conference on Machine Learning*, 2023.
- [18] H. Guo, T. H. Nguyen, and A. Yadav, “CounterNet: End-to-end training of prediction aware counterfactual explanations,” *Proceedings of the 29th ACM SIGKDD Conference on Knowledge Discovery and Data Mining*, 2021.
- [19] R. Guidotti, “Counterfactual explanations and how to find them: literature review and benchmarking,” *Data Mining and Knowledge Discovery*, vol. 38, pp. 2770 – 2824, 2022.